Performance improvement in nanoparticle-assisted stimulated-emission-depletion nanoscopy

Yonatan Sivan

Related Articles

Superradiance from one-dimensionally aligned ZnO nanorod multiple-quantum-well structures
Appl. Phys. Lett. 100, 233118 (2012)

Two-photon-pumped optical gain in dye-polymer composite materials
Appl. Phys. Lett. 100, 133305 (2012)

Two-photon-pumped optical gain in dye-polymer composite materials
APL: Org. Electron. Photonics 5, 83 (2012)

Stimulated emission in AlGaN/AlGaN quantum wells with different Al content
Appl. Phys. Lett. 100, 081902 (2012)

Microwave-induced spin-flip scattering of electrons in point contacts
Low Temp. Phys. 37, 925 (2011)

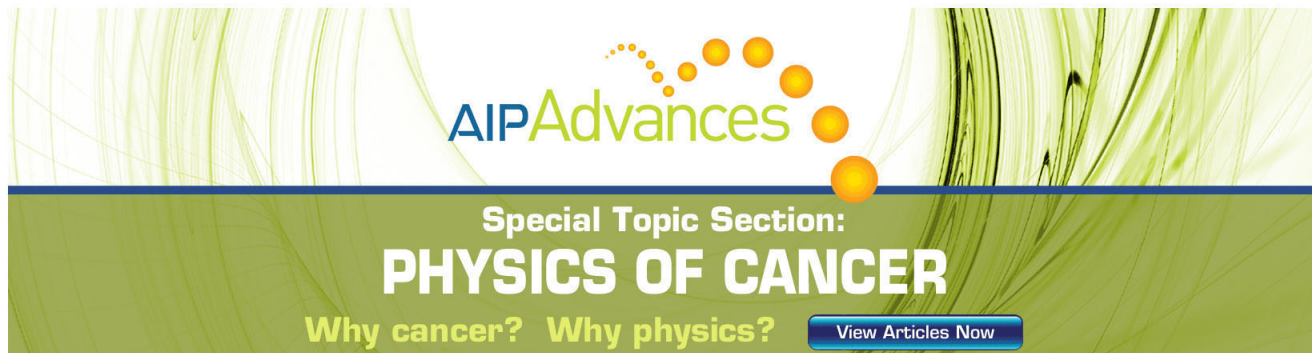## Additional information on Appl. Phys. Lett.

Journal Homepage: http://apl.aip.org/
Journal Information: http://apl.aip.org/about/about_the_journal
Top downloads: http://apl.aip.org/features/most_downloaded
Information for Authors: http://apl.aip.org/authors

Performance improvement in nanoparticle-assisted stimulated-emission-depletion nanoscopy

Yonatan Sivan[a)]

The Blackett Laboratory, Department of Physics, Imperial College London, London SW7 2AZ, United Kingdom

We revisit stimulated-emission-depletion (STED) nanoscopy theory for the case when metal nanoparticles are used to improve the nanoscope's performance. We show that the improved performance can be estimated in a simple way with no need for heavy computations. We then systematically study the dependence of the improved performance on the field and decay rate enhancements, as well as on the STED pulse and time-gating durations. © 2012 American Institute of Physics. [http://dx.doi.org/10.1063/1.4735319]

Tremendous progress has been achieved in recent years in breaking the diffraction limit in optical far-field imaging. Specifically in fluorescence microscopy, several techniques providing diffraction-unlimited resolution were developed.[1,2] The most prominent of these is probably stimulated-emission-depletion (STED) nanoscopy, which offers superb resolution along with fast acquisition times.[3,4] In a typical STED nanoscope, a focused excitation beam is spatially overlapped with a doughnut-shaped beam[5,6] that de-excites emitters to the ground state everywhere except for within the center of the doughnut.[7] STED nanoscopy has been performed in a pulsed depletion scheme,[3,4] a lower intensity continuous wave (CW) depletion scheme,[8] and even a time-gated scheme.[9–11] Despite this progress and diversity, the STED nanoscope, however, has still not become a wide-spread tool, mainly because of the high intensities and complicated setup required and the nanoscope's high cost.[12] In addition, STED can especially benefit from improved brightness and photo-stability of the fluorescent emitters.

Recently, we proposed that hybrid fluorescent labels consisting of a metal nanoparticle (NP) and a fluorescent emitter (or emitters) can improve the performance of the STED nanoscope.[13,14] Specifically, we predicted that this technique, which we call nanoparticle-assisted STED (NP-STED) nanoscopy, can improve the resolution, or alternatively and more likely, reduce the intensity requirements from the STED pulse. NP-STED can also reduce photobleaching by several mechanisms: reduced STED powers result in weaker singlet and triplet photo-bleaching,[6] shorter excited singlet state lifetime results in reduced singlet photo-bleaching,[15,16] and possibly, the huge resonant decay rate enhancements may be tuned to quench the triplet population and further reduce triplet photo-bleaching.[17] While the principles of NP-STED were explained in detail and demonstrated for one possible design of the hybrid label by Sivan *et al.*,[13] a detailed study of the dependence of the improved performance on the temporal configuration of the STED nanoscope and on the NP properties was lacking. This letter is dedicated to the detailed study of these dependencies.

The theory of STED resolution was worked out in detail by Leutenegger *et al.*[7] who showed that the probability of spontaneous emission in the presence of a depleting beam is given by

$$\eta_{SP}(r - r_0) = \phi \frac{1 + \gamma(r - r_0)e^{-k_{S_1} t_{STED}(1 + \gamma(r - r_0))}}{1 + \gamma(r - r_0)}. \quad (1)$$

Here, r is the coordinate in the image space, r_0 is the scan coordinate (i.e., the center of the illumination and STED beams), and ϕ is the quantum yield of the emitter. The depletion factor is given by

$$\gamma(r - r_0) = \frac{\zeta(r - r_0)k_{vib}}{\zeta(r - r_0)k_{S_1} + k_{vib}}, \quad (2)$$

where

$$\zeta(r - r_0) = \frac{I_{STED}(r - r_0)}{I_{sat}}, \quad I_{sat} = \frac{hc\,k_{S_1}}{\lambda_{STED}\sigma_{em}(\lambda_{STED})}, \quad (3)$$

is the STED intensity normalized by the saturation intensity, a level at which the rate of stimulated emission equals the total rate of spontaneous decay of the excited singlet state,[18] k_{S_1}. Additional parameters used above are the depletion wavelength λ_{STED}, the emission cross-section σ_{em}, the vibrational decay rate k_{vib}, the STED pulse duration T_{STED}, and $hc \approx 2 \cdot 10^{-25}$ Jm. Equation (1) was derived under two conditions, $1/T_{STED} \ll k_{vib}$ and $k_{S_1} \ll k_{vib}$, which hold in basically all STED configurations to date and for any value of STED intensity.

Assuming a doughnut-shape beam, $I_{STED}(r) = \frac{4P_{STED}}{\pi w^4}r^2 e^{-2r^2/w^2}$, it can be shown that, Γ_{res}, the resolution improvement with respect to the diffraction limit is given by[10]

$$\Gamma_{res} \cong \sqrt{1 + p(1 + k_{S_1}T_G - e^{-\alpha + k_{S_1}T_G})}, \quad p = \frac{P_{STED}}{P_{sat}}, \quad (4)$$

where $P_{STED} = \int I_{STED}(r)d^2r$ is the STED power, $P_{sat} = \frac{\pi w^2}{4}I_{sat}$ is the saturation power, $\alpha \equiv k_{S_1}T_{STED}$ is the ratio of the STED pulse duration and the excited singlet state lifetime, and T_G is the time-gate duration; the latter is the time

[a)]E-mail: ysivan@imperial.ac.uk.

window after the end of the depletion pulse during which any arriving photons are discarded.

The dependence of the resolution improvement (4) on its various parameters is demonstrated in Figs. 1(a) and 1(b). The parameter α defines two regimes of interest: for STED pulses, which are short with respect to the excited singlet level lifetime (i.e., when $\alpha \ll 1$),[4,6] spontaneous emission during the STED pulse is negligible, so that the spontaneous emission probability (1), hence, the resolution improvement (4), depend on the depletion intensity I_{STED} but not on k_{S_1}. In this case, the resolution improvement, given by $\Gamma_{res} \cong \sqrt{1 + p\alpha}$, is optimal and resolution improvement by time-gating is negligibly small.[10] As the STED pulses become longer, spontaneous emission can compete with stimulated emission and cause the depletion to be less effective. Eventually, in the CW-STED limit[8] ($\alpha \gg 1$), the resolution improvement is given by $\Gamma_{res} \cong \sqrt{1 + p}$, i.e., it depends on both I_{STED} and k_{S_1}.

Nevertheless, the time-gate duration T_G can be used to remove the dependence of Γ_{res} on k_{S_1} and thus counteract the limitation a fast spontaneous decay puts on the resolution improvement.[9–11] In order to understand how this happens, recall that during the STED pulse, the excited-state population decreases due to both stimulated and spontaneous emission. Thus, the excited state population decays faster in the depleted regions, which are the regions corresponding to the outer wings of the excitation spot. Accordingly, the contribution of these regions to the fluorescence signal is diminishing with the STED duration, an effect which is responsible for the resolution improvement. In fact, since photons are spontaneously emitted at a uniform rate, but from regions of increasingly different populations, then, for $T_G = T_{STED}$ (i.e., when any spontaneously emitted photons arriving before the end of the STED pulse are discarded), the dependence of the spontaneous emission probability (1) and resolution improvement (4) on the decay rate k_{S_1} is effectively removed and the optimal (i.e., k_{S_1}-free) resolution of the $\alpha \ll 1$ case is restored. For CW-STED, i.e., when $\alpha \gg 1$ (so that necessarily $T_G < T_{STED}$), the dependence on k_{S_1} is only partially removed. In this case, the resolution improvement with optimal time-gating is given by $\Gamma_{res} \cong \sqrt{1 + p(1 + k_{S_1} T_G)}$. Clearly, time-gating comes at the cost of a weaker signal:[10,11] it decays as $\sim e^{-k_{S_1} T_G}$. Accordingly, to date, only modest durations of time-gating were employed;[9,11] those allowed to improve the resolution by up to about a factor 2.

The introduction of metal NPs to STED nanoscopy has several effects. First, tuning the plasmon resonance to the depletion wavelength leads to a local enhancement of the depletion intensity experienced by the emitters, denoted by Γ_I. In that regard, the depletion power which is focused on the emitters is used in a more efficient manner, effectively increasing the power of the STED beam. Specifically, $I_{STED}(r - r_0) \rightarrow \Gamma_I(r, r_0; \lambda_{STED}) I_{STED}(r - r_0)$, so that the intensity enhancement will vary now with both the scan coordinate r_0 and the sample space coordinate r (i.e., the intensity will no longer be translation-invariant). At the same time, the decay rate of the excited singlet level is enhanced as well, by a factor denoted as Γ_k, so that $k_{S_1} \rightarrow \Gamma_k(r, \lambda_{em}) k_{S_1}$. Accordingly, the decay rate depends now strongly on the emitter position with respect to the metal NP as well as on the emission wavelength λ_{em}. When the decay rate enhancement is dominated by the absorption in the metal, there is also a reduction of the apparent quantum yield.

As an example of these effects, let us recall the gold nano-shell particles studied in Ref. 13. Whereas, in general, $\Gamma_I = \Gamma_I(r, r_0; \lambda_{STED})$, it can be shown that for emitters placed at the NP core, the field enhancement depends only very weakly on the illumination pattern.[19] Thus, in particular, the field enhancement depends only very weakly on the scan coordinate, $\Gamma_I(r = 0, r_0; \lambda_{STED}) \cong \Gamma_I(\lambda_{STED})$, so it would be well justified to take the average enhancement level over the scan coordinate as a characteristic value. In what follows, we denote this average value by $\bar{\Gamma}_I(\lambda_{STED})$. Fig. 2(b) shows that the spectral dependence of the averaged intensity enhancement follows a distinct resonant form. Fig. 2(c) shows that although Γ_k reaches very high values at resonance, still, $\Gamma_k(\lambda_{em}) < 200$, i.e., the enhancement at the center of the emission line λ_{em} remains much lower.[20] These two enhancement effects correspond to an effective rescaling of the normalized STED power by $\Gamma_p \equiv \bar{\Gamma}_I(\lambda_{STED})/\Gamma_k(\lambda_{em})$. One can verify that the enhancement of the averaged normalized power is by $\Gamma_p \sim 8$ for the 50 nm nano-shell particles whereas $\Gamma_p \sim 1$ for the particles of 20–25 nm size. The associated reduction in quantum yield, shown in Fig. 2(d), has a relatively weak spectral dependence in all three geometries.

We would now like to study how the performance improvement offered by NP-STED depends on the STED intensity enhancement $\bar{\Gamma}_I(\lambda_{STED})$ and decay rate enhancement $\Gamma_k(\lambda_{em})$, as well as on the STED pulse duration and on the time-gating. Hybrid metal NP-emitter fluorescent labels can be made with a wide variety of geometries, material
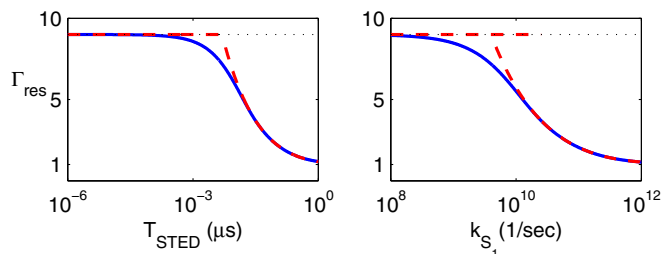

FIG. 1. Improved resolution (4) offered by STED nanoscopy at fixed STED pulse energy without (solid blue) and with (dotted black) time-gating ($T_G = T_{STED}$) as a function of (a) STED pulse duration and (b) spontaneous decay rate. Also shown are the analytic approximations for the pulsed and CW regime (dashed red). The former is indistinguishable from the case of time-gating.
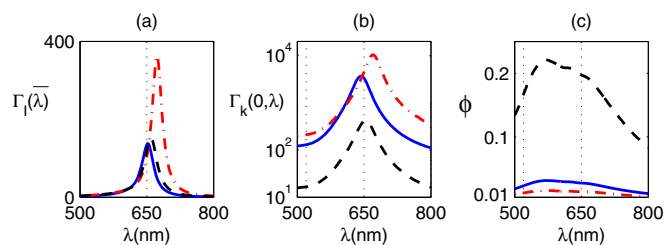

FIG. 2. Optical parameters for silica-gold nanoshells of sizes 52 nm (dashed black line), 26 nm (blue solid line), and 20 nm (dash-dotted red line). (a) Averaged intensity enhancement, (b) decay rate enhancement at core center, and (c) apparent quantum yield as a function of wavelength.

compositions, and spectral configurations. In order to avoid specifying those details and to be able to describe any such hybrid label in a single plot, we assume the specified field and decay rate enhancements to represent the averaged values experienced by the emitter(s) in the given label. Specifically, the decay rate enhancement should be viewed as that for a single emitter or the average for a spatial distribution of many emitters; the intensity enhancement should be viewed as the average over the scan coordinate. In some typical cases, e.g., metal nanoshells or small spheres, such an average intensity enhancement can be easily extracted from the quasistatic solution for a plane wave illumination.[19] Under these conditions, Eq. (4) provides a measure of the system's resolution (i.e., the width of the point-spread-function), although the illumination pattern is no longer strictly translation-invariant. This averaging also removes the need for intensive computations of the interactions of the doughnut beam with the scaterrer.[13,19] The resolution improvement offered by NP-STED can then be simply calculated from Eq. (4) as $\Gamma_{res}^{NP-STED}/\Gamma_{res}^{STED}$ where the STED resolution serving as reference is set to be $\Gamma_{res}^{STED} \sim 6$ for the pulsed configuration and $\Gamma_{res}^{STED} \sim 3-4$ for the CW configurations. Such resolutions are provided by commercially available STED nanoscopes. In practice, the size of the NP limits the best resolution achievable. Accordingly, if the resolution calculated from Eq. (4) is smaller than the NP size, as would typically occur for sufficiently high field enhancements (see e.g., the upper parts of all the subplots in Fig. 3), one should exploit the (residual) field enhancement in order to lower the STED intensity. For brevity, we refer below only to resolution improvement and only plots of the resolution improvement are shown here. However, it can be easily shown that the potential STED intensity reduction is given, to a good approximation, by $(\Gamma_{res}^{NP-STED}/\Gamma_{res}^{STED})^2$.

For pulsed STED operation ($T_{STED} = 250$ ps), Fig. 3(a) shows that when the decay rate enhancement is small, the field enhancement provides a clear improvement of resolu-

tion and almost no sensitivity to the decay rate enhancement, manifested by the small slope of the constant resolution improvement contours. Thus, in this regime, there is improvement of resolution (or equivalently, a reduction of required intensity) for any level of field enhancement even if it is smaller than the decay rate enhancement, i.e., even for particles for which $\Gamma_p < 1$. However, once the decay rate enhancement becomes sufficiently high, it clearly limits the resolution improvement. In this case, the slope of the constant resolution improvement contours grows from 0 to 1. Similarly, the contour slope is 1 also in the CW-STED regime (see Fig. 3(b)), in which case improved resolution can be attained only when the field enhancement dominates the decay rate enhancement (i.e., only for $\Gamma_p > 1$).

The improved performance in time-gated NP-STED is demonstrated in Figs. 3(c) and 3(d). For pulsed STED, time-gating removes the dependence on the decay rate and enables to exploit the intensity enhancement in its full extent for resolution improvement. However, as noted above, one should bear in mind that a high decay rate enhancement may not only be accompanied by a reduction of signal due to a more effective gating but also possibly by a further reduced quantum yield. This is also relevant for the CW case, see Fig. 3(d).

According to the discussion above, we can identify two scenarios for the use of metal NPs in STED nanoscopy, depending on the value of Γ_p. NPs for which $\Gamma_p \sim 1$ or lower should be used only in pulsed STED. In this case, the resolution improvement originates purely from near-field enhancement, whereas enhancement of the decay rate enhancement affects mostly the signal level, if at all. In the second scenario, NPs for which $\Gamma_p > 1$ (such as the 50 nm gold nano-shells studied in Ref. 13) can be used either in pulsed or CW-STED. In both cases, it is preferable to work with STED pulses as short as about 50–100 ps (see Fig. 1). While it is well known that such short pulses provide optimal resolution, they have also the disadvantage of providing strong photobleaching due to the high intensities. As NP-STED allows using lower peak intensities, one could benefit from the optimal resolution without the penalty of lower photostability. In addition, pulses of that duration are readily available from supercontinuum sources, with no need for further temporal streching.[21]

Clearly, one would like to use metal NPs as small as possible with Γ_p as large as possible. In that regard, since NP-STED relies on local field enhancement, it would provide improved performance also with few nm particles for which the (far-field) cross-sections are undetectable with standard optical microscopy. Thus, one can use NPs, which are as small as possible in order to minimize the interference with the biological processes and in order to maximize the label density and attain optimal resolution. This is a major advantage over existing microscopy techniques that rely on metal NPs.[22] On the other hand, it should be noted that upon scaling down of their size, nano-shells exhibit increasing decay rate enhancements but no further field enhancement (which is roughly uniform within the core for such small nano-shells). Accordingly, Γ_p diminishes for smaller shells. However, particles where the emitters lie out of the metal particle may benefit also from further field enhancement when the particle size is decreased, and thus, could maintain
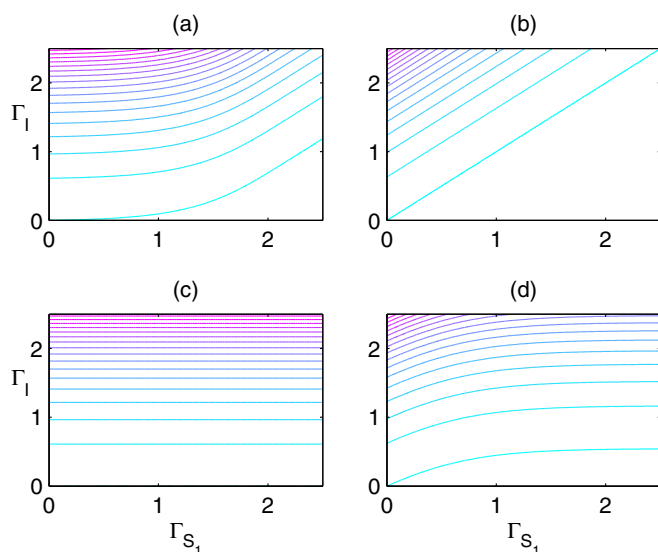

FIG. 3. Contour maps (ranging from 1 to 15 in steps of 1) of resolution improvement provided by NP-STED compared with standard STED for (a) pulsed operation ($T_{STED} = 250$ ps and $p \sim 700$), (b) CW-STED ($p \sim 10$), (c) time-gated pulsed STED ($T_G = T_{STED} = 250$ ps and $p \sim 700$), and (d) time-gated CW-STED ($T_G = 2$ ns and $p \sim 10$). In all cases, $1/k_{S_1} = 5$ ns.

a high Γ_p at small sizes; possibly, such particles may even benefit from a favourable spectral dependence of the quantum yield away from resonance. Nevertheless, since the decay rate enhancement becomes very high even far from resonance at few nm emitter-metal separations, it would be challenging to fabricate metal NPs that resonate at the long wavelength regime of the visible spectrum, which have $\Gamma_p > 1$ and are smaller than about 10 nm. Yet, while fluorescent labels of of 10–20 nm sizes may not be suitable for inner-cell studies, such NPs can find many uses in microscopy. Indeed, similar NPs of comparable size are currently used as fluorescent or contrast labels in microscopy; most notably of those are functionalized quantum dots,[23] Cornell (C)-dots,[24] and nano-diamond particles with nitrogen vacancy color centers.[25–27]

In conclusion, the performance improvement offered by attaching fluorescent emitters to metal NPs has been studied in detail, with emphasis on the optimal temporal configuration. These results would be useful in guiding the experimental tests of the performance improvement by the NP-STED technique and the development of cheap, low intensity STED sources.[12]

[1]S. Hell, Science **316**, 1153 (2007).
[2]W. Moerner, Proc. Natl. Acad. Sci. U.S.A **104**, 12596 (2207).
[3]S. Hell and J. Wichmann, Opt. Lett. **19**, 780 (1994).
[4]T. Klar, S. Jakobs, M. Dyba, A. Egner, and S. Hell, Proc. Natl. Acad. Sci. U.S.A **97**, 8206 (2000).
[5]P. Török and P. Munro, Opt. Express **12**, 3605 (2004).
[6]G. Donnert, J. Keller, R. Medda, M. Andrei, S. Rizzoli, R. Luhrman, R. Jahn, C. Eggeling, and S. Hell, Proc. Natl. Acad. Sci. U.S.A **103**, 11440 (2006).
[7]M. Leutenegger, C. Eggeling, and S. Hell, Opt. Express **18**, 26417 (2010).
[8]K. Willig, B. Harke, R. Medda, and S. Hell, Nat. Methods **4**, 915 (2007).
[9]E. Auksorius, B. Boruah, C. Dunsby, P. Lanigan, G. Kennedy, M. Neil, and P. French, Opt. Lett. **33**, 113 (2008).
[10]J. Moffitt, C. Osseforth, and J. Michaelis, Opt. Express **19**, 4242 (2011).
[11]G. Vicidomini, G. Moneron, K. Han, V. Westphal, H. Ta, M. Reuss, J. Engelhardt, C. Eggeling, and S. Hell, Nat. Methods **8**, 571 (2011).
[12]S. Schrof, T. Staudt, E. Rittweger, N. Wittenmayer, T. Dresbach, J. Engelhardt, and S. Hell, Opt. Express **19**, 8066 (2011).
[13]Y. Sivan, Y. Sonnefraud, S. Kéna-Cohen, J. Pendry, and S. Maier, ACS Nano **6**, 5291 (2012).
[14]F. Balzarotti and F. Stefani, ACS Nano **6**, 4580 (2012).
[15]J. Enderlein, Appl. Phys. Lett. **80**, 315 (2002).
[16]J. Enderlein, Phys. Chem. Chem. Phys. **4**, 2780 (2002).
[17]S. Kéna-Cohen, A. Wiener, Y. Sivan, P. Stavrinou, D. Bradley, A. Horsefield, and S. Maier, ACS Nano **5**, 9958 (2011).
[18]Note that for a non-ideal emitter for which the quantum yield is lower than 100%, the total spontaneous decay consists of contributions from both radiative and non-radiative decay channels.
[19]M. Foreman, Y. Sivan, S. A. Maier, and P. Török, "Illumination-dependence of plasmonic near-field enhancements," J. Opt. Sco. Am. A (submitted).
[20]In that regard, we should note that while the condition $1/T_{STED} \ll k_{vib}$ mentioned above holds in general, the decay rate enhancement induced by the metal may, in principle, put the validity of the second condition, $k_{S_1} \ll k_{vib}$, in question. However, the spectral scheme in NP-STED, whereby the plasmon resonance of the metal NP is tuned to the depletion wavelength, minimizes the decay rate enhancement at the emission wavelength. Consequently, the second condition should hold in NP-STED as well. In cases where the decay rate enhancement is even more significant, one should use a more general expression for the depletion efficiency (Ref. 7).
[21]D. Wildanger, E. Rittweger, L. Kastrup, and S. Hell, Opt. Express **16**, 9614 (2008).
[22]S. Maier, *Plasmonics: Fundamentals and Applications* (Springer, 2007).
[23]M. Bruchez, M. Moronne, P. Gin, S. Weiss, and A. Alivisatos, Science **281**, 2013 (1998).
[24]A. Burns, H. Ow, and U. Wiesner, Chem. Soc. Rev. **35**, 1028 (2006).
[25]O. Faklaris, V. Joshi, T. Irinopoulou, P. Tauc, M. Sennour, H. Girard, C. Gesset, J.-C. Arnault, A. Thorel, J.-P. Boudou, P. Curmi, and F. Treussart, ACS Nano **3**, 3955 (2009).
[26]C. Fu, H. Lee, K. Chen, T. Lim, H. Wu, P. Lin, P. Wei, P. Tsao, H. Chang, and W. Fann, Proc. Natl. Acad. Sci. U.S.A. **104**, 727 (2007).
[27]K. Han, K. Willig, E. Rittweger, F. Jelezko, C. Eggeling, and S. Hell, Nano Lett. **9**, 3323 (2009).